



MAX-PLANCK-GESELLSCHAFT

# Intercomparison of HONO SCDs from MAX-DOAS observations during the MAD-CAT campaign

Yang Wang (1, 2), Thomas Wagner (1), Pinhua Xie (2), Julia Remmers (1), Ang Li (2), Johannes Lampel (3, 1), Udo Friess (3), Enno Peters (4), Folkard Wittrock (4), Andreas Richter (4), Andreas Hillboll (4), Rainer Volkamer (5), Ivan Ortega (5), Francois Hendrick (6), Michel Van Roozendael (6), Junli Jin (7), Jianzhong Ma (7), Hang Su (8), Yafang Cheng (8)

- (1) Satellite group, Max Planck Institute for Chemistry, Mainz, Germany
- (2) Anhui Institute of Optics and Fine Mechanics, Chinese Academy of Sciences, Hefei, China
- (3) Institute of Environmental Physics, University of Heidelberg, Heidelberg, Germany
- (4) Institute of Environmental Physics, University of Bremen, Bremen, Germany
- (5) Department of Chemistry and Biochemistry, University of Colorado, Boulder, CO, USA
- (6) Belgian Institute for Space Aeronomy, Brussels, Belgium
- (7) Chinese Academy of Meteorological Sciences, Beijing, China
- (8) Multiphase Chemistry Department, Max Planck Institute for Chemistry, Mainz, Germany



MAX-PLANCK-INSTITUT FÜR CHEMIE

## SUMMARY

In order to promote the development of the passive DOAS technique the Multi Axis DOAS – Comparison campaign for Aerosols and Trace gases (MAD-CAT) was held at the Max Planck Institute for Chemistry in Mainz, Germany from June to October 2013. During this campaign we present intercomparison results for tropospheric slant column densities (SCDs) of nitrous acid (HONO) retrieved by seven research groups using same baseline DOAS fit parameters.

### Intercomparison:

The standard deviation (SD) and mean deviation of HONO dSCD for all participants from the reference are quite small, mostly less than  $\pm 0.4 \times 10^{15}$  molec/cm<sup>2</sup> close to the fit error. And for the days with high HONO concentration, the correlation coefficients and slopes of linear regression are close to unity with quite small intercept for low elevation angles (EA). In general good agreement of the resulting HONO dSCD sets was found.

### Sensitivity studies:

The overall systematic uncertainty of about  $-1.9$  to  $2.9 \times 10^{15}$  molec/cm<sup>2</sup> is much larger than the random uncertainty of  $\pm 0.4 \times 10^{15}$  molec/cm<sup>2</sup>. The uncertainties from fit wavelength ranges and polynomials take most part of the systematic uncertainty. The errors of cross sections of O<sub>4</sub>, Ring, NO<sub>2</sub> and the probable H<sub>2</sub>O absorption around 364 nm are secondary important systematic error sources.

## INTERCOMPARISON

### 1) Baseline fit Parameters:

The DOAS fit parameters used for intercomparison is shown in Table 1 based on the suggestions in Hendrick et. al, 2014. The Fig. 1 shows the wavelength-dependence typical optical depths (OD) of the trace gases related to the HONO fit. The DOAS fit sample from Hefei instrument in Fig. 2 shows the absorption of HONO can be retrieved. To detect the tropospheric species, the Fraunhofer reference spectrum (FRS) can be a zenith spectrum from each measurement sequence or around noon on each day. The results using two types of FRS are compared between the groups, respectively.

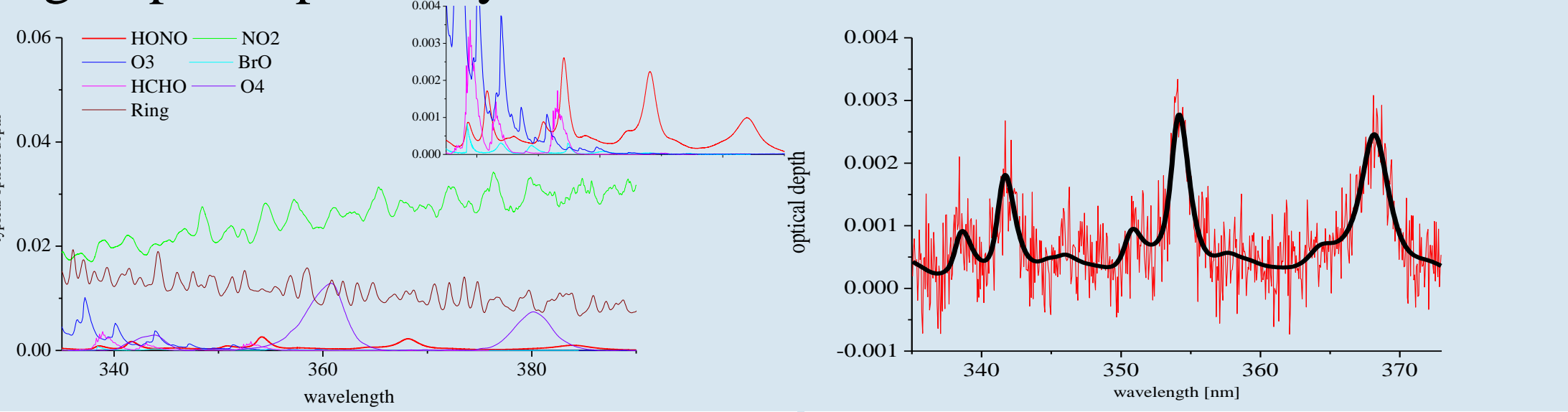


Fig. 1. The wavelength-dependence typical optical depths of the trace gases in the HONO fit

Parameter	Specification
Fitting interval	335-373
Wavelength calibration	Calibration based on reference solar NDSC (air)
Cross sections (air)	Stutz et al. (2000), 296 K
HONO	Vandaele et al. (1998), 220 K and 296 K convolved with 10 correction ( $1 \times 10^{17}$ molecules/cm <sup>2</sup> )
NO <sub>2</sub>	Taylor series approach to compensate the wavelength-dependence of AMF (Pukite et al. 2010)
O <sub>3</sub>	Bogumil et al. (2003), 223 K and 243 K convolved with 10 correction ( $1 \times 10^{20}$ molecules/cm <sup>2</sup> )
BrO	Fleischmann et al. (2004), 223 K
O <sub>4</sub>	Hermann et al., 2003
HCHO	Meller and Moortgat (2000), 293 K
Ring effect	From DOASIS for the reference spectrum at noon on 18 June 2013
Intensity offset	The additional ring spectrum: ring $\times 4$
Polynomial term	Quadratic offset
Wavelength adjustment	Polynomial of order 5
FRS	All spectra shifted and stretched against reference spectrum

Table 1. Baseline DOAS fit parameters for intercomparison

Instrument	Group	Type of Spectrometer / Camera	Grade of Instrument
Erivmes MAX-DOAS	IUP, Heidelberg	Avantes ULS	Scientific grade
MAXDOAS	BIRA-IASB	Oriel MS2601 / Roper 1340x400	Scientific grade
BedDOM MAX-DOAS	IUP, Bremen	Shamrock 3031 Roper 1300x400	Scientific grade
2D-MAX-DOAS	Hefei, CAS	Action SP2500S	Scientific grade
2D-MAX-DOAS	CU-Boulder	Action SP2150 PIXIS 400	Scientific grade
4scimath-MAX-DOAS	MPIC	Andor	Scientific grade
mini-MAX-DOAS	Beijing, CMA	ocean optics usb 2000	Mini DOAS

Table 2. The instruments participating in the intercomparison

Seven MAX-DOAS instruments in Table 2 from Germany, American and Chinese groups participate the HONO intercomparison. Fig. 3 shows the period coverage and time resolution of the instruments in the time interval of the intercomparison from 12 June to 5 August, 2013 (162 - 185 day). The fitting error of HONO dSCDs from MPIC is relative larger than other scientific grade instruments because of its short exposure time of about 6 seconds. The fitting error from Beijing mini-MAX-DOAS is reasonable larger than other scientific grade instruments. The sky conditions identified by Hefei MAX-DOAS using the classification scheme (Wagner et al, 2014 and Wang, et al, 2015) are shown in Fig. 5 for the whole comparison period.

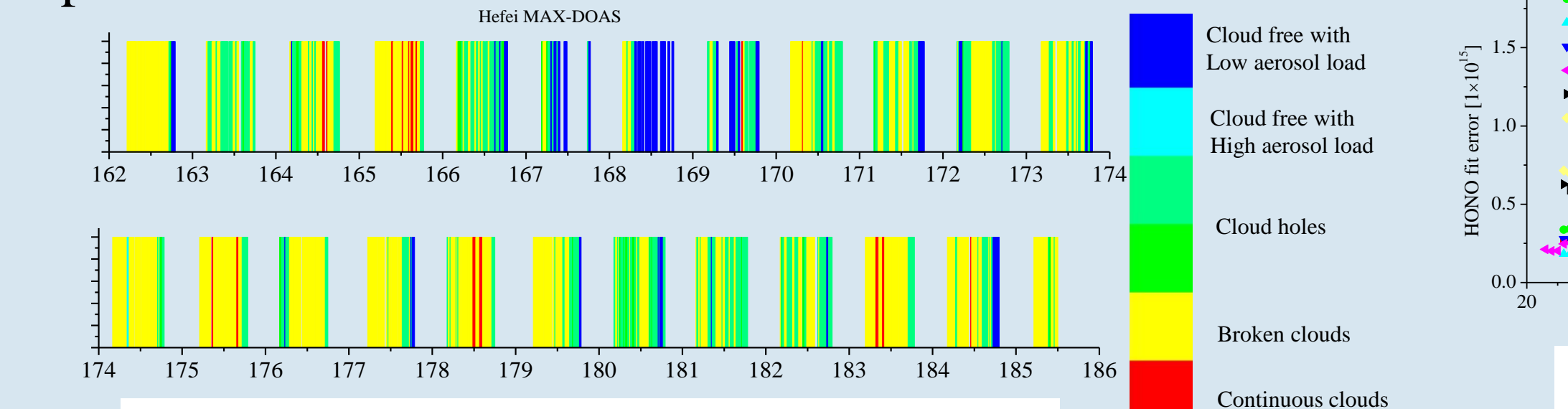


Fig. 3. Period coverage and time resolution of the instruments

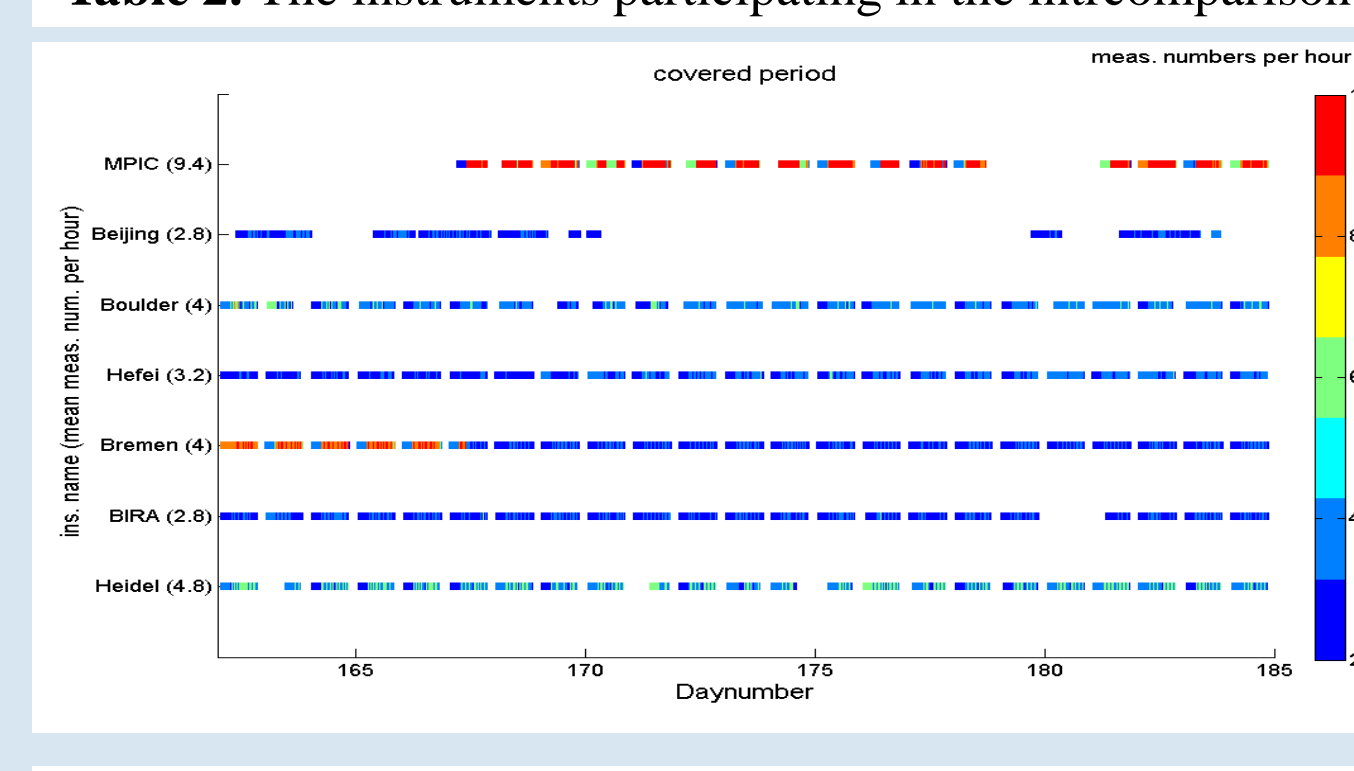


Fig. 4. The SZA gridded mean HONO dSCD fit errors and normalized errors from different MAX-DOAS

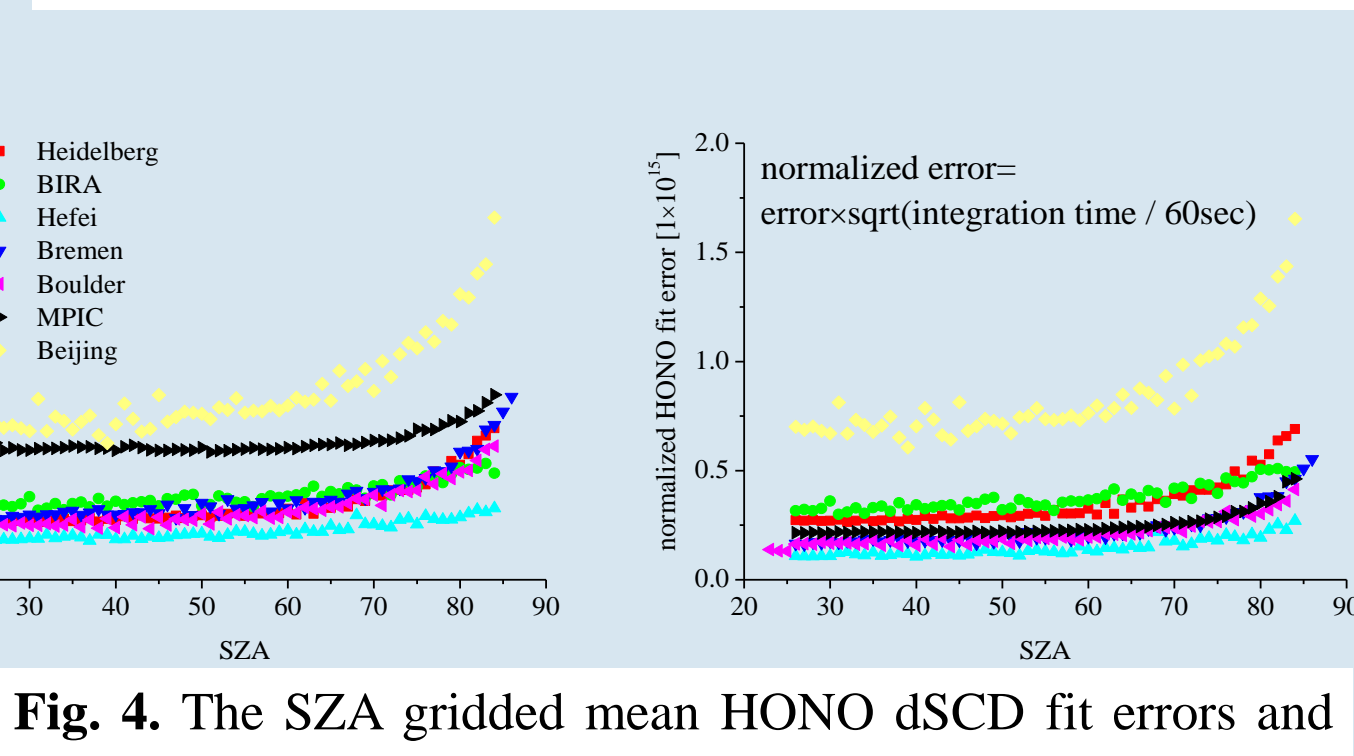


Fig. 5. Sky conditions identified by Hefei MAX-DOAS

### 3) Intercomparison for the results with sequential FRS:

HONO dSCDs retrieved by each group are averaged over periods of one hour. A apparent good agreement between the instruments is found in Fig. 6. A reference data set was created by averaging data from four instruments (Heidelberg, BIRA, Hefei and Bremen). In Fig. 7 all the instruments have a symmetric and quasi-Gaussian shape statistic histogram of the deviations of HONO dSCD from the reference, but some differences in the standard deviation (SD) and mean deviation ( Fig. 8), which are quite small, mostly less than  $\pm 0.4 \times 10^{15}$  molec/cm<sup>2</sup> close to the fit error in Fig. 4. The Largest SD is found for MPIC, consistent with its larger noise level. The largest positive and negative mean deviation are found for Boulder and Bremen, respectively.

For eight days with high HONO dSCD, the linear regressions of the HONO dSCD against the reference are shown in Fig. 8 and 9 for each group and each EA. All the instruments compare well with the reference for low EAs. For EA of 1° correlation coefficients (R) are close to unity, slopes deviate by no more than 18% and intercepts are less than  $0.4 \times 10^{15}$  molec/cm<sup>2</sup>. The deprivations of R and slope along the increase of EA are due to the lower HONO dSCDs than the fit errors for high EA.

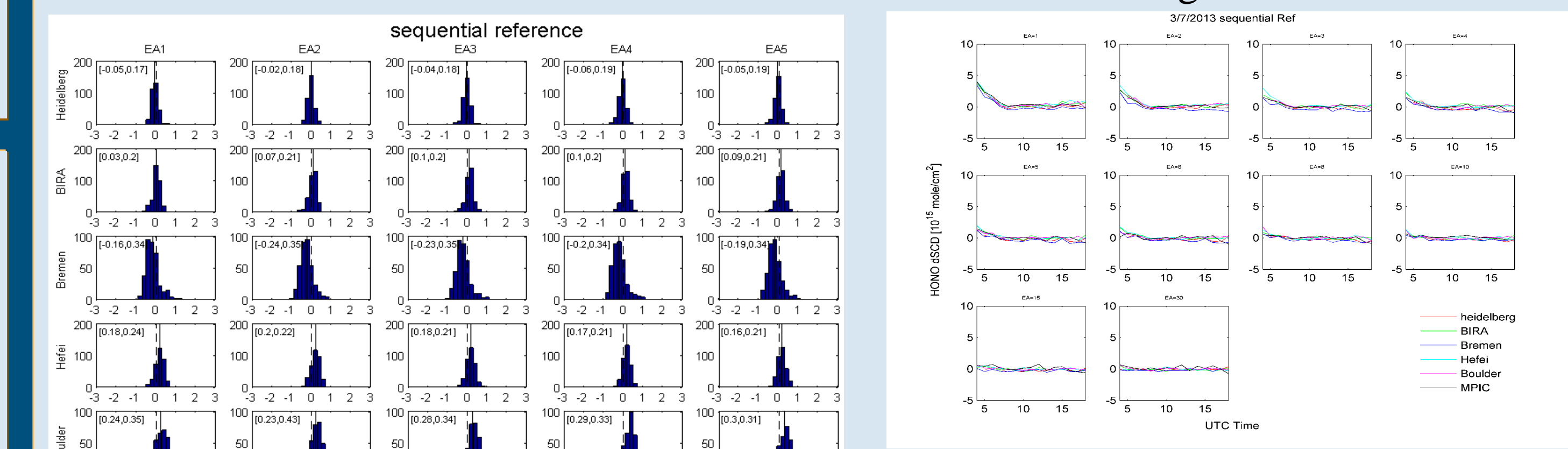


Fig. 6. An example of the diurnal evolution of the hourly mean HONO dSCDs

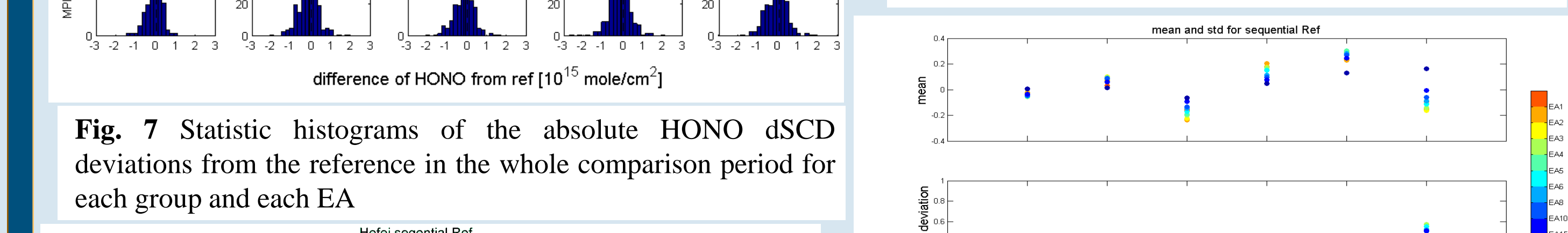


Fig. 7. Statistic histograms of the absolute HONO dSCD deviations from the reference in the whole comparison period for each group and each EA

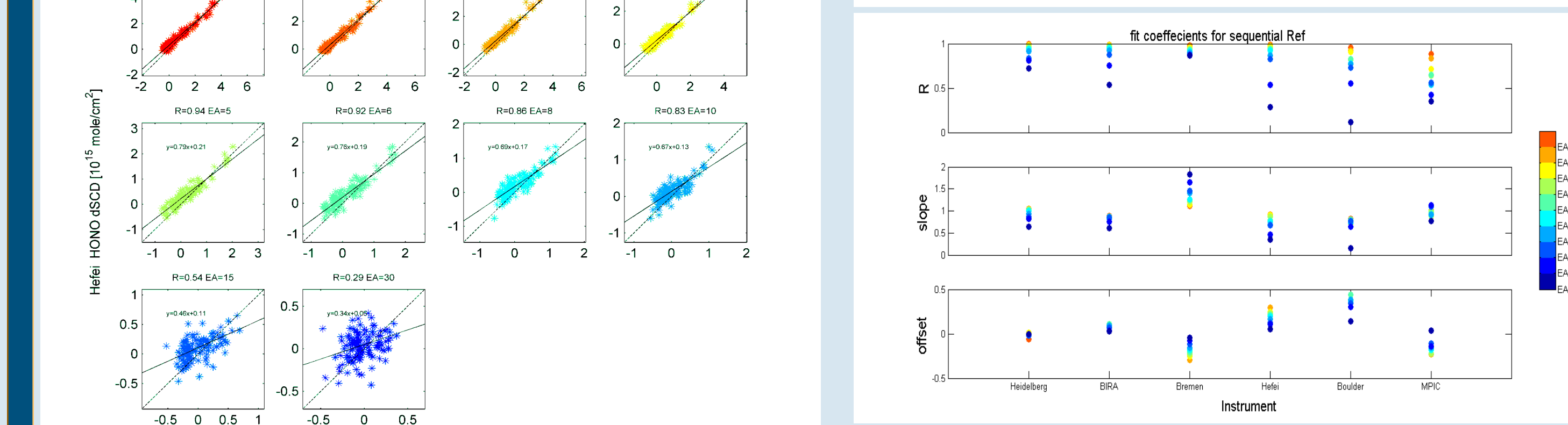


Fig. 8. Upper two: standard deviations and mean values of the HONO dSCDs deviations from the reference; bottom three: the correlation parameters of linear regressions of the HONO dSCDs against the reference for each group and each EA.

Fig. 9 Linear regressions of the HONO dSCDs against the reference for each EA for Hefei MAX-DOAS

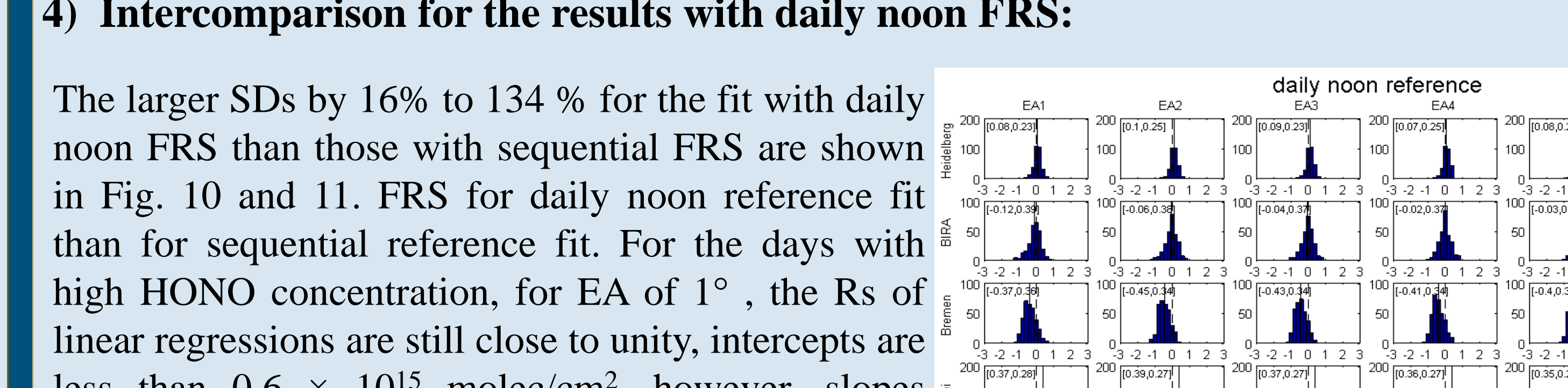


Fig. 9. Linear regressions of the HONO dSCDs against the reference for each EA for Hefei MAX-DOAS

### 4) Intercomparison for the results with daily noon FRS:

The larger SDs by 16% to 134 % for the fit with daily noon FRS than those with sequential FRS are shown in Fig. 10 and 11. FRS for daily noon reference fit than for sequential reference fit. For the days with high HONO concentration, for EA of 1°, the Rs of linear regressions are still close to unity, intercepts are less than  $0.6 \times 10^{15}$  molec/cm<sup>2</sup>, however, slopes deviate by up to 28% in Fig. 11. So using FRS close to measurement spectrum can improve the stability and accuracy of HONO retrieval. Note the much larger SD for Beijing mini-MAX-DOAS is due to the worse ratio of signal to noise than other scientific grade MAX-DOAS. Fortunately for low EA, the Rs and slopes close to unity and small intercept of linear regression indicate mini-MAX-DOAS is capable to observe HONO.

Fig. 10 the statistic histograms of the absolute HONO dSCD deviations from the reference in the whole comparison period for each group and each EA.

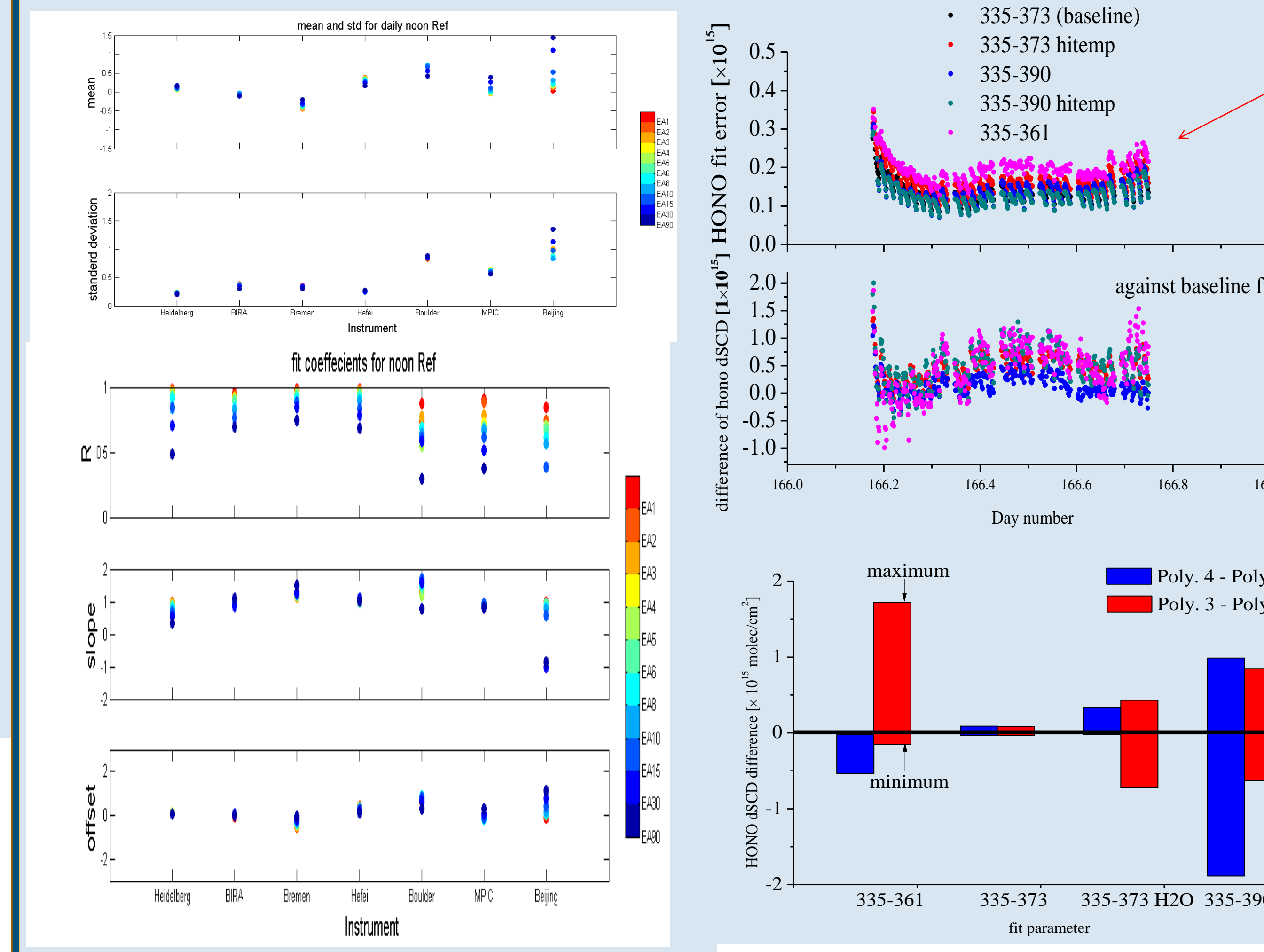


Fig. 11 same with Fig. 8, but for the fit with daily noon FRS

## SENSITIVITY STUDIES

Two days of 16 and 18 June with low and high HONO concentration are selected to analyze sensitivities of HONO dSCD on fit parameters using Hefei MAX-DOAS data.

- Wavelength interval: in 335 – 361 or 335 – 390 nm, HONO dSCDs are mostly larger by up to  $2 \times 10^{15}$  molec/cm<sup>2</sup> than in 335-373 of the baseline fit shown in Fig. 12.
- Considering the typical optical depth in Fig. 1, NO<sub>2</sub>, Ring and O<sub>4</sub> are the most important interferences of HONO retrieval. The interferences of the three items to the HONO retrieval in 335-390 nm are smallest in the three wavelength ranges shown in Fig. 13.
- The HONO dSCD differences between polynomials of degrees of 3 to 5 are larger in 335-361 and 335-390 shown in Fig. 14. Including the H<sub>2</sub>O cross section in the fit will activate its dependence on polynomials in 335-373.
- The strong fit residual around 364 nm are probably from water vapor absorption indicated by the similar structure of the fit residual with the H<sub>2</sub>O cross sections from hitemp (Rothman et al., 2010) and BT2 (Barber et al., 2006) right shifted by 1.4 nm in Fig. 15. The retrieved ODs of a variety of trace gases in 335-390 nm by the fit including hitemp H<sub>2</sub>O cross section are appreciably different from those by the fits excluding H<sub>2</sub>O cross section shown in Fig. 16. About  $1 \times 10^{15}$  molec/cm<sup>2</sup> larger of HONO dSCD is found for the fits including H<sub>2</sub>O, and the differences of HONO dSCDs between both of the fits are ideally linear related to the retrieved H<sub>2</sub>O dSCDs shown in Fig. 17.
- The estimations of dominant systematic uncertainties are shown in Table 3. The uncertainties from fit wavelength ranges and polynomials of degrees of 3 to 5 take most part of the total systematic uncertainty.

Dominant systematic uncertainties	estimation of HONO dSCD uncertainty ( $\times 10^{15}$ molecules/cm <sup>2</sup> )
wavelength range	-1 to 2
possible H <sub>2</sub> O	-0.1 to 0.8
polynomial	-0.5 to 1.8 (337-361); -0.2 to 0.5 (335-373 with H <sub>2</sub> O), 0 to 0.1 (334-373 without H <sub>2</sub> O); -0.6 to 1 (335-390 with H <sub>2</sub> O)
ring source	-1 to 0.7
O <sub>4</sub> cross section	-1 to 0 (stronger when including H <sub>2</sub> O)
HONO cross section	0.25 (HONO dSCD of 5) according to 5% relative uncertainty (Stutz et al., 2000)
variation of slit function	about 0.1 for the changing of slit function by 5% (HONO dSCD of 5)
NO <sub>2</sub> AMF wavelength dependence	-0.1 to 0.1
Total	-1.9 to 2.9

Table 3. The estimations of systematic uncertainties of HONO dSCD retrieval

Fig. 12 Top: the HONO fit errors in different wavelength ranges; bottom: the differences of HONO dSCDs from the substitutable fits with those from the baseline fit. Note "hitemp" means the hitemp H<sub>2</sub>O cross sections included in the fit

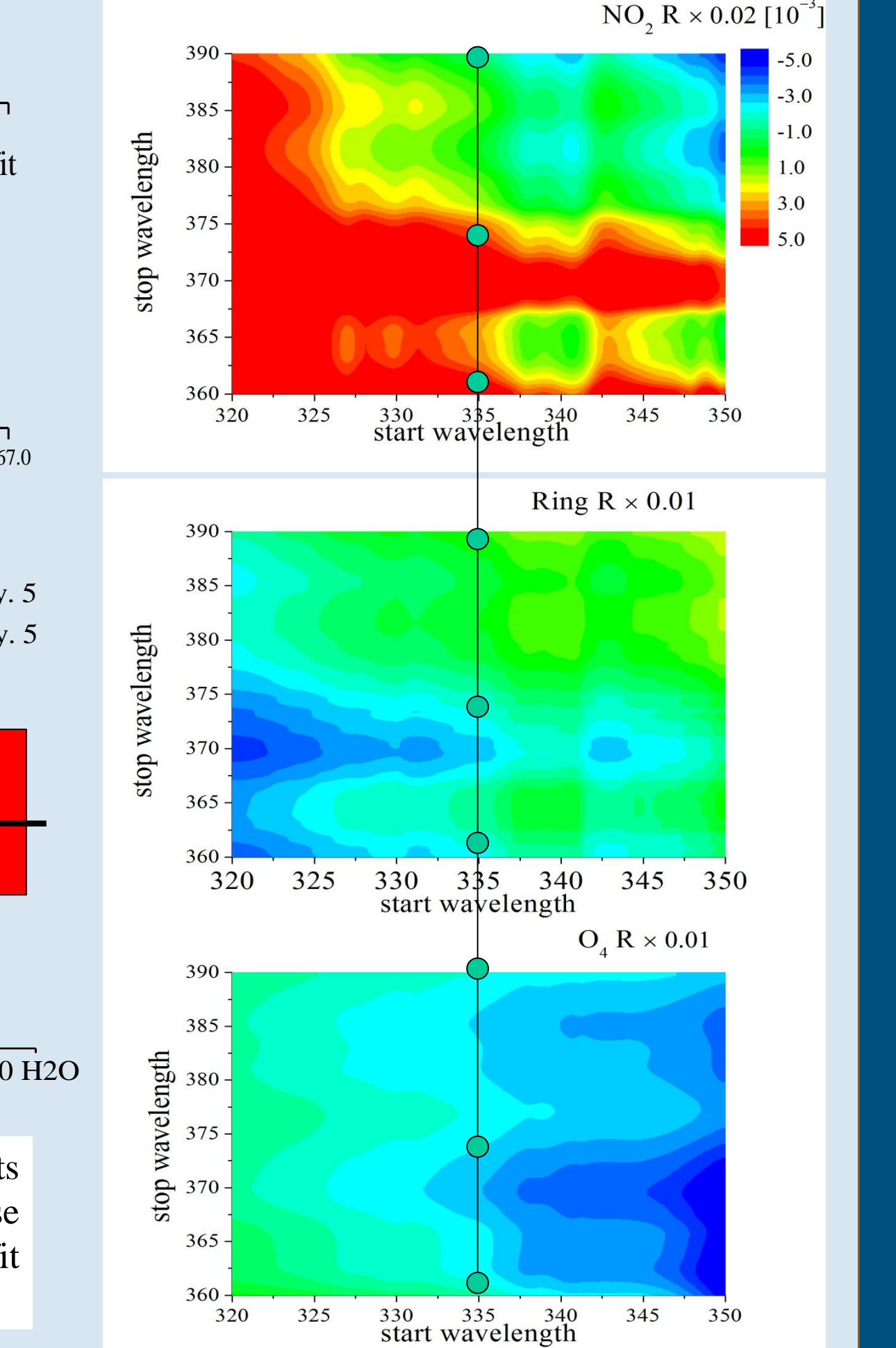


Fig. 12 Top: the HONO fit errors in different wavelength ranges; bottom: the differences of HONO dSCDs from the substitutable fits with those from the baseline fit. Note "hitemp" means the hitemp H<sub>2</sub>O cross sections included in the fit

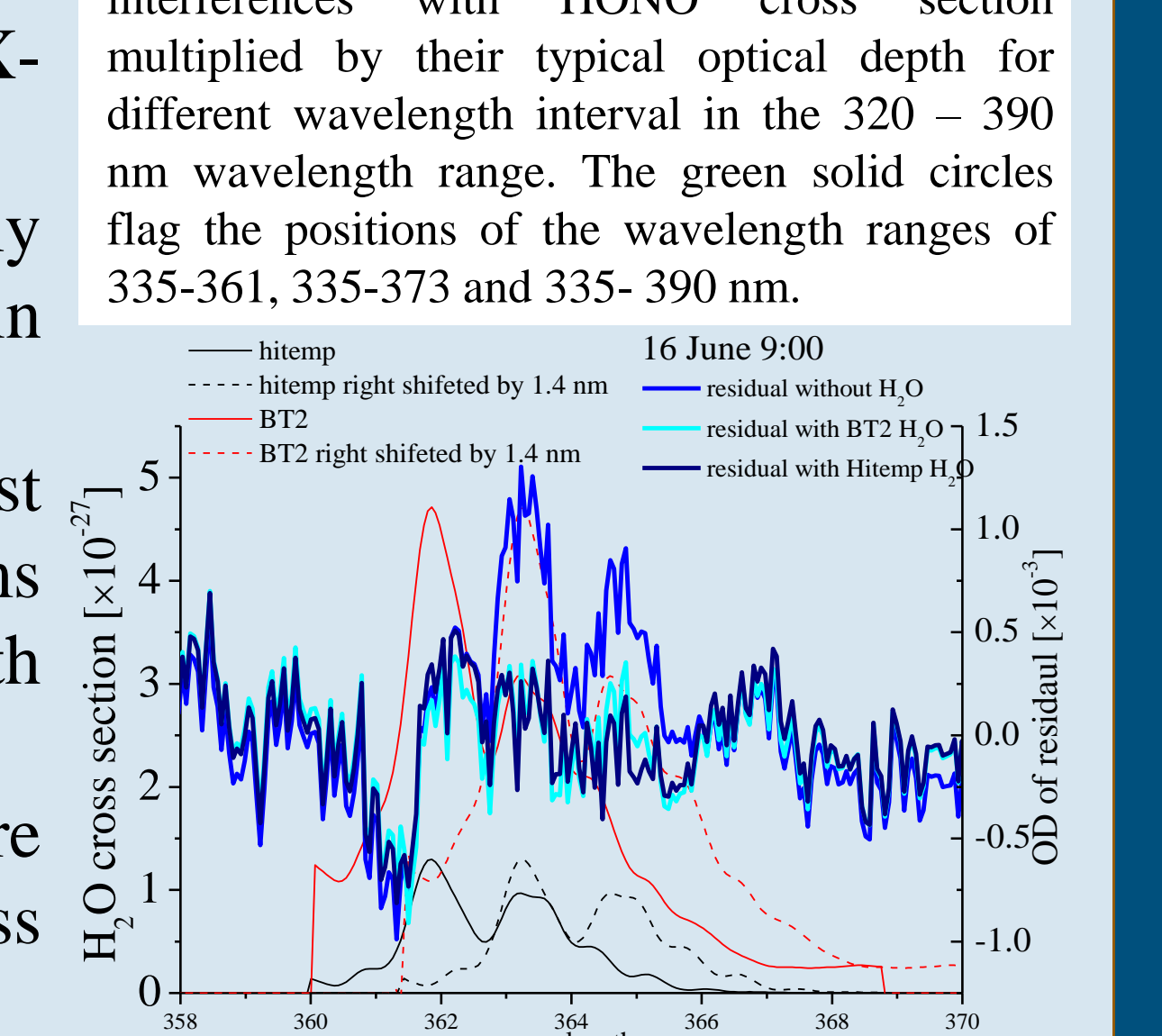


Fig. 13 correlation coefficients of the three interferences with HONO cross section multiplied by their typical optical depth for different wavelength interval in the 320 – 390 nm wavelength range. The green solid circles flag the positions of the wavelength ranges of 335-361, 335-373 and 335- 390 nm.

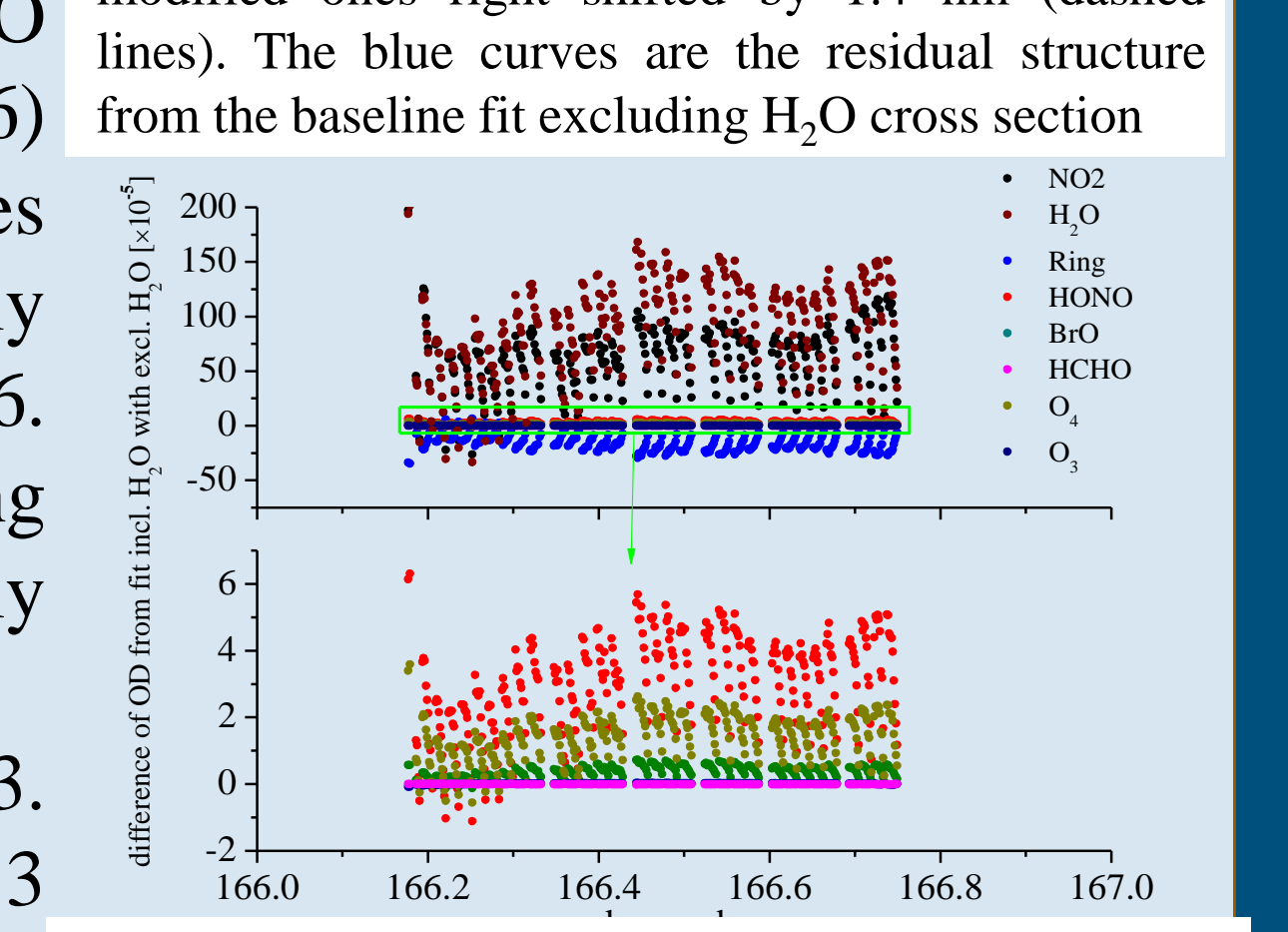


Fig. 14 Differences of HONO dSCDs from the fits including the polynomials of order 3 and 4 with those including the polynomial of order 5 in four fit parameter sets

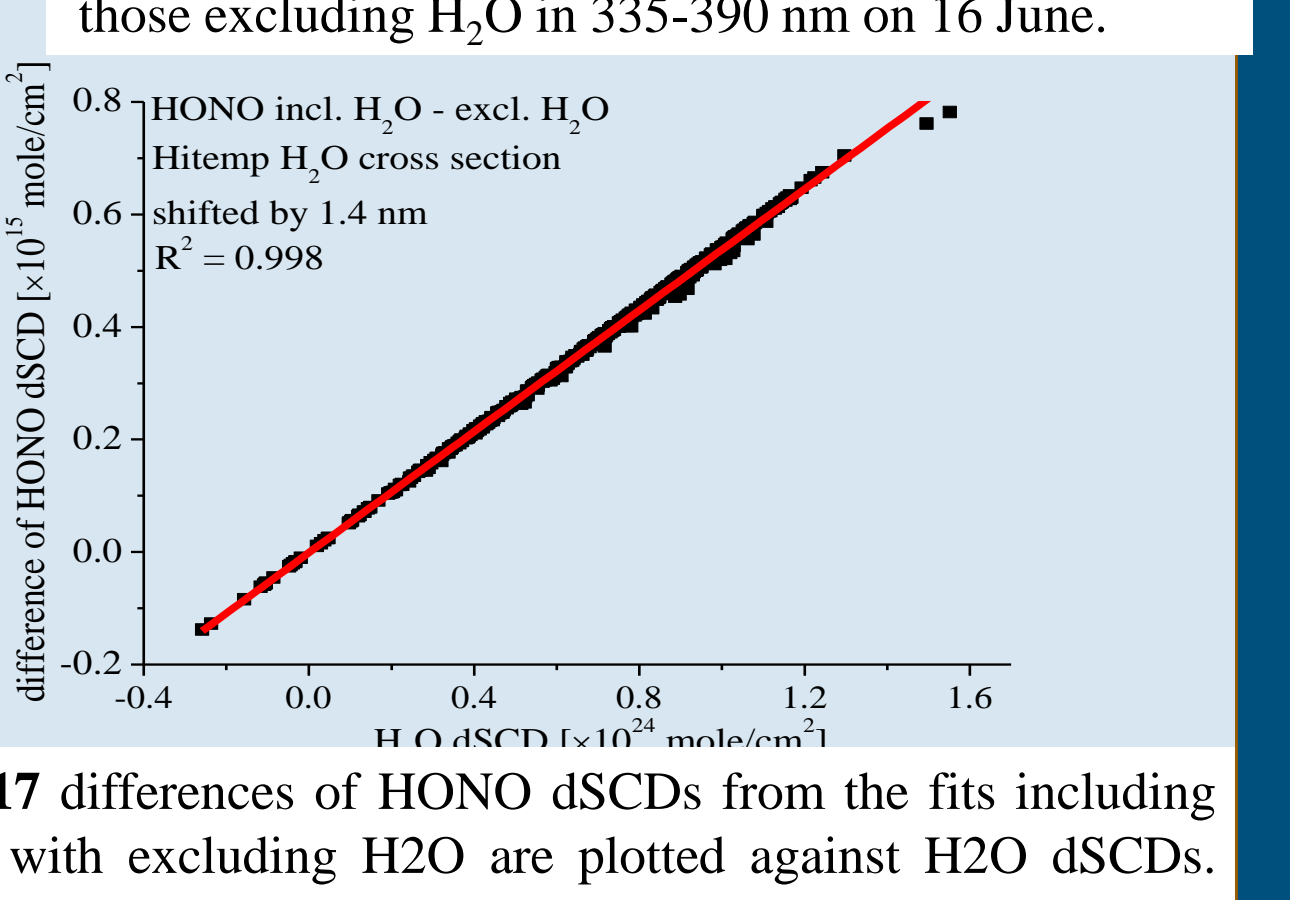


Fig. 15 H<sub>2</sub>O cross sections (solid lines) and modified ones right shifted by 1.4 nm (dashed lines). The blue curves are the residual structure from the baseline fit excluding H<sub>2</sub>O cross section

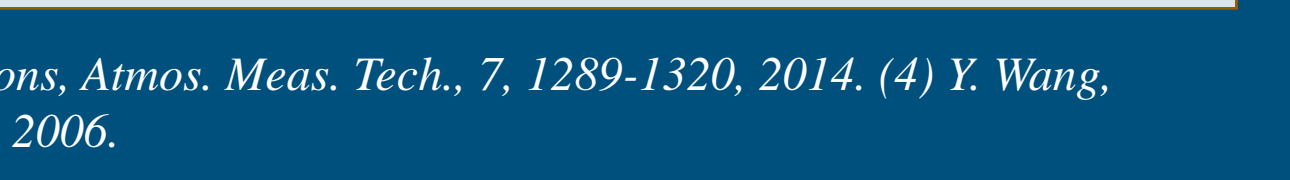


Fig. 16 differences of the OD of a variety of trace gases from the fits including H<sub>2</sub>O cross section with those excluding H<sub>2</sub>O in 335-390 nm on 16 June.



Fig. 17 differences of HONO dSCDs from the fits including H<sub>2</sub>O with excluding H<sub>2</sub>O are plotted against H<sub>2</sub>O dSCDs. The red line is the linear regression of the dots.

(1) Pukite, G., Köhl, S., Deutschmann, T., et al.: Extending differential optical absorption spectroscopy for limb measurements in the UV. Atmos. Meas. Tech., 3, 631–653, 2010. (2) Hendrick, E., Müller, J. F., Clemer, K., et al.: Four years of ground-based MAX-DOAS observations of HONO and NO<sub>2</sub> in the Beijing area. Atmos. Chem. Phys., 14, 765–781, 2014. (3) Wagner, T., Beirle, S., Dörner, S., Friess, et al.: Cloud detection and classification based on MAX-DOAS observations. Atmos. Meas. Tech., 7, 1289–1320, 2014. (4) Y. Wang, M. Penning de Vries, P. H. Xie, et al.: Cloud and aerosol classification for 2 1/2 years of MAX-DOAS observations in Wuxi (China) and comparison to independent data sets, submitted to AMT, 2015. (5) Rothman, L. S., et al.: HITRAN, the high-temperature molecular spectroscopic database. Journal of Quantitative Spectroscopy and Radiative Transfer 111.15, 2139–2150, 2010. (6) Barber R.J., et al.: A high-accuracy computed water line list, Mon Not R Astron Soc., 368: 1087–94, 2006.